Engineering 7 (2021) 1064–1075

Contents lists available at ScienceDirect

Engineering

journal homepage: www.elsevier.com/locate/eng

Research
Active Support of Power System to Energy Transition—Article

Research on DC Protection Strategy in Multi-Terminal Hybrid HVDC System

Yuping Zheng [a,c], Jiawei He [b,*], Bin Li [b,*], Tonghua Wu [a,c,*], Wei Dai [a], Ye Li [b]

[a] State Key Laboratory of Smart Grid Protection and Control, State Grid Electric Power Research Institute (NARI Group Corporation), Nanjing 211106, China
[b] Key Laboratory of Smart Grid of Ministry of Education, Tianjin University, Tianjin 300072, China
[c] College of Energy and Electrical Engineering, Hohai University, Nanjing 210098, China

ARTICLE INFO

Article history:
Received 5 June 2020
Revised 2 February 2021
Accepted 29 March 2021
Available online 24 May 2021

Keywords:
Multi-terminal hybrid HVDC system
Single-ended protection
Transient information
Active injection

ABSTRACT

Multi-terminal hybrid high-voltage direct current (HVDC) systems have been developed quickly in recent years in power transmission area. However, for voltage-source converter (VSC) stations in hybrid HVDC systems, no direct current (DC) filters are required. In addition, the DC reactor is also not installed at the line end because the DC fault can be limited by the converter itself. This means that the boundary element at the line end is absent, and the single-ended protections used in line commutated converter (LCC) based HVDC (LCC-HVDC) systems or VSC-HVDC systems cannot distinguish the fault line in multi-terminal hybrid HVDC systems. This paper proposes a novel single-ended DC protection strategy suitable for the multi-terminal hybrid HVDC system, which mainly applies the transient information and active injection concept to detect and distinguish the fault line. Compared with the single-ended protections used in LCC-HVDC and VSC-HVDC systems, the proposed protection strategy is not dependent on the line boundary element and is thus suitable for the multi-terminal hybrid HVDC system. The corresponding simulation cases based on power systems computer aided design (PSCAD)/electromagnetic transients including DC (EMTDC) are carried out to verify the superiority of the proposed protection.

1. Introduction

In recent years, there has been widespread application of high-voltage direct current (HVDC) transmission systems in the field of power transmission because of its outstanding advantages, such as large transmission capacity, long transmission distance, and low power loss [1,2]. However, the traditional HVDC system, namely, the line commutated converter (LCC) based HVDC (LCC-HVDC) system, has the essential drawback of commutation failure because the used thyristor is half-controlled. Differently, the voltage-source converter (VSC) has no commutation failure problem because of the application of full-controlled power electronic switches, for example, the insulated gate bipolar transistor (IGBT) [3]. Nevertheless, the application of full-controlled power electronic switches will lead to a significantly higher economic investment. Therefore, the hybrid HVDC system, which generally applies the LCC at the rectifier terminal and the VSC at the inverter terminal, has the potential for widespread application in the HVDC transmission area, because it can significantly reduce the risk of commutation failure compared with LCC-HVDC systems, and reduce the required investment compared with VSC-HVDC systems [4].

Generally, there are four types of hybrid HVDC system, that is, the pole-to-pole hybrid system, hybrid multi-infeed system, terminal-to-terminal hybrid system, and multi-terminal hybrid system [5]. The pole-to-pole hybrid system and hybrid multi-infeed system can provide reactive power for alternating current (AC) systems by the introduced VSC, and it can thus significantly reduce the commutation failure probability of the LCC [5]. The terminal-to-terminal hybrid system uses the LCC at the rectifier side, and the VSC at the inverter side, which can completely prevent commutation failure (the commutation failure mainly occurs at the inverter side) [5]. Furthermore, the multi-terminal hybrid system can realize the multi-terminal power supply, thus having wide application potential in the HVDC transmission area. However, the protection of multi-terminal hybrid HVDC systems is a challenge for its engineering application.

* Corresponding authors.
E-mail addresses: hejiawei_tju@126.com (J. He), binli@tju.edu.cn (B. Li), wutonghua@sgepri.sgcc.com.cn (T. Wu).

https://doi.org/10.1016/j.eng.2021.05.002

The direct current (DC) protections in LCC-HVDC or VSC-HVDC systems can be considered for using in multi-terminal hybrid HVDC systems. In general, the single-ended protections are mainly used as the primary protection for the DC line in HVDC systems owing to the consideration of operation speed. In LCC-HVDC systems, the single-ended protections based on the fault traveling wave are used as the primary protection for the DC line [6,7]. For example, the company ABB proposed to use the change value and rate of change of voltage traveling wave to distinguish the internal fault and external fault in LCC-HVDC systems. The company Siemens used the change value and rate of change of DC voltage in the protection criterion. Both of the above-mentioned protections distinguish the internal and external faults based on the obstacle effect of the DC filter on the fault traveling wave. In addition, in VSC-HVDC systems, DC reactors will be installed at both terminals of each DC line, which also has an obstacle effect on the fault traveling wave. Therefore, the single-ended protections used in LCC-HVDC system are also suitable for VSC-HVDC systems. Furthermore, considering that the higher the frequency the greater will be the obstacle effect of the DC reactor [8], the single-ended protection based on high-frequency transient voltage (or current) was proposed for the VSC-HVDC system to improve the ability against high transition resistance [8–11].

However, it should be noted that the above-mentioned single-ended protections are all based on the obstacle effect of the line boundary elements on the fault traveling wave, such as the DC reactor and DC filters [6–11]. However, in the multi-terminal hybrid HVDC system, DC filters are not required for the VSC station. In addition, the DC reactor may only be installed at the converter exit because the multi-terminal hybrid HVDC system primarily uses converters to eliminate and limit the DC fault current, and there is a reduced requirement on the fault current limiting reactor. This indicates that the boundary element at the line terminal is absent. Under this condition, the single-ended DC protections used in the LCC-HVDC and VSC-HVDC systems are no longer suitable. The current differential protection is not dependent on the line boundary, which, however, is severely affected by the line distribution capacitor current, and requires the communication facility. In summary, the DC protection strategy suitable for multi-terminal hybrid HVDC systems, particularly the single-ended one, still needs to be researched further.

In this study, a novel DC protection strategy which is based on the transient variable and active injection concept is proposed for the multi-terminal hybrid HVDC system. The content of this paper is organized as follows. In Section 2, the typical topology of the multi-terminal hybrid HVDC system is introduced, based on which the applicability of the existing single-ended DC protections is discussed. Then, the DC protection strategy suitable for the multi-terminal hybrid HVDC system is proposed in Section 3. In Section 4, the corresponding simulation cases are performed to verify the feasibility and superiority of the proposed protection. Finally, Section 5 presents the conclusions of the study.

2. Challenge of protection in multi-terminal hybrid HVDC system

2.1. Typical topology of multi-terminal hybrid HVDC system

There has been widespread application of LCC-HVDC systems in practical engineering. However, the LCC is composed of half-controlled thyristors. As is commonly known, while the thyristor can be turned on based on control, its turned-off operation is uncontrollable. This means that the commutation between the bridge arms in the LCC is highly dependent on the AC-system voltage. When the AC-system voltage drops, the commutation between the bridge arms may fail. In engineering practice, the commutation failure of the LCC has become the core technical problem of the LCC-HVDC system, particularly at the inverter side [12].

In contrast, the VSC is composed of full-controlled power electronic switches, such as the IGBT, and thus have no commutation failure problem. Therefore, hybrid HVDC systems, where the VSC is applied to replace the LCC at the inverter side and where the LCC is still used at the rectifier side, have been applied to the HVDC transmission technique, because it can prevent the commutation failure problem and enhance the interconnected AC system stability [5].

Fig. 1 shows a typical three-terminal hybrid HVDC transmission system, which will be quickly put into operation in China [13]. As shown in Fig. 1, the rectifier station S_3 in the hybrid system applies the LCC, while the converter stations S_1 and S_2 apply the modular multilevel converters (MMCs). In this way, the commutation failure problem can be avoided effectively as most of the commutation failure problems occur on the inverter side [5].

In addition, the LCC can itself eliminate the DC fault current by adjusting the trigger angle. However, the conventional VSC, such as the two-level VSC and the half-bridge MMC, does not have any fault-handling capability. Therefore, in the hybrid HVDC system, the hybrid MMC, which consists of half-bridge sub-modules (HBSMs) and full-bridge sub-modules (FBSMs) [14–17], is applied to stations S_1 and S_2, as shown in Fig. 1. After the DC fault, the capacitors in the FBSMs are inserted into the fault circuit in reverse to the fault current by turning off the FBSMs. Therefore, the DC fault current can be eliminated quickly. Then, the fault part in the system can be cut off by the corresponding switches (SW_1–SW_3), which does not have DC fault arc extinguishing capability.

2.2. Challenge of DC line protection in multi-terminal hybrid HVDC system

In general, the DC protections in LCC-HVDC systems or VSC-HVDC systems are considered for use in multi-terminal hybrid HVDC systems. However, they cannot be directly applied owing to the absence of the boundary element at the line end.

For example, in LCC-HVDC systems, the smoothing reactor and DC filter are installed at the line end. Owing to the obstacle effect of the reactor and filter, the fault traveling wave under the external fault condition is noticeably smaller than that under the internal fault condition. Therefore, the traveling-wave based protections, which are widely used in LCC-HVDC systems, can use the amplitude or rate of change of the voltage traveling wave (or of the voltage) to distinguish the internal fault and external fault reliably.

In the VSC-HVDC system, the waveform quality of the MMC is much better than the LCC in the LCC-HVDC system, so the filters are not required anymore. However, in VSC-HVDC systems, a large DC reactor will be installed at each line end to limit the DC fault current. This means that the line boundary still exists, and thus the DC protection can still distinguish the fault line reliably.

However, in multi-terminal hybrid HVDC systems, the DC fault current can be limited and eliminated by the converters. This means that the requirement on the DC reactor for fault current limitation is reduced significantly. As shown in Fig. 1, in the multi-terminal hybrid HVDC system, the DC reactors are only installed at the converter exits, and not at the line end. Moreover, for the VSC, the DC filter is no longer required because the output waveform quality is good enough. Under this condition, the traditional single-ended DC protection cannot distinguish the fault line anymore. For example, for the protection P_2 installed at the exit of station S_2, the observed fault traveling wave after the fault f_1 ($Line_1$ end) is almost the same as that after the fault f_4 ($Line_2$ end). This

means that when only the local-measured traveling wave is used, the protection P_2 cannot distinguish the faults f_1 and f_4.

In summary, the single-ended protections used in LCC-HVDC or VSC-HVDC systems cannot be used in multi-terminal hybrid HVDC systems directly. And the single-ended protection, which is suitable for multi-terminal hybrid HVDC systems, should be researched further.

3. Proposed DC protection strategy for multi-terminal hybrid HVDC system

3.1. Proposed protection strategy

According to the above-mentioned analysis, the single-ended protections for the LCC-HVDC and VSC-HVDC systems cannot be directly used in the multi-terminal hybrid HVDC system owing to the absence of the boundary elements (such as the DC filter and DC reactor) at the line end. Therefore, in this study, a novel single-ended protection strategy that can reliably distinguish the fault line without a boundary element is proposed, as shown in Fig. 2 (mainly referring to the protection P_1 (in Fig. 1) at the station S_1, which is connected with multiple DC lines). The detailed steps are as follows.

(1) Measure the DC voltages and currents, that is, the DC voltage at the line side of the reactor at station S_1 (U_{dc1_l}), the DC voltage at the station side of the reactor at station S_1 (U_{dc1_s}), the DC current from bus to $Line_1$ (I_{dc12}), and the DC current from bus to $Line_2$ (I_{dc13}). If $|dU_{dc1\_l}/dt| > \Delta_1$ or $|dI_{dc12}/dt| > \Delta_2$ or $|dI_{dc13}/dt| > \Delta_2$ (t represents the time; Δ_1 and Δ_2 are the threshold values of the start criterion; and U_{dc1_l}, U_{dc2_l}, and U_{dc3_l} are the DC voltage at the line side of the reactor at stations S_1, S_2, and S_3, respectively), the protection is started.

(2) Extract the high-frequency components of the DC voltages U_{dc1_l} and the DC voltage at the station side of the reactor at station S_1 (U_{dc1_s}), that is, $U_{dc1\_l\_hf}$ and $U_{dc1\_s\_hf}$.

If $\max|U_{dc1\_l\_hf}|/\max|U_{dc1\_s\_hf}| \le k_{set}$ (k_{set} is the reliability coefficient, which is a little larger than 1), it indicates that the fault happens at the converter station S_1. Block the converter, then open the switch SW_3 after the fault current is cleared. And the protection algorithm is ended.

If $\max|U_{dc1\_l\_hf}|/\max|U_{dc1\_s\_hf}| > k_{set}$, it indicates that the fault happens at the DC side of the reactor (installed at the converter exit). Block the converter. But the protection algorithm is not ended, and the following steps will be implemented.

(3) Delay Δt_1, then inject a controlled current from the converter (research into the current injection method will be presented below). Delay Δt_2. Δt_1 and Δt_2 are threshold values of the delay times.

(4) The fault line can be distinguished according to the DC current.

If the DC current on $Line_1$ is larger than the threshold value, namely, $I_{dc12} > I_{set}$, it indicates that the fault is on $Line_1$. Block the converter again, then open the switch SW_1. After that, restart the converter. The protection is ended.

If the DC current on $Line_1$ is not larger than the threshold value, namely, $I_{dc12} \le I_{set}$, but the DC current on $Line_2$ is greater than the threshold value, namely, $I_{dc13} > I_{set}$, it indicates that the fault is on $Line_2$. Under this condition, block the converter again, then open the switch SW_2. Subsequently, restart the converter. And the protection algorithm is ended.

If neither I_{dc12} nor I_{dc13} is larger than the threshold value I_{set}, it indicates that the fault is nonpermanent and has disappeared. The converter can be restarted directly. The protection is ended.

Δ_1 should be larger than the rate of change of DC voltage that may occur during system normal operation, and Δ_2 should be larger than the rate of change of DC current that may occur during system normal operation. The delay time Δt_1 is introduced to guarantee the insulation recovery of the fault line under the nonpermanent fault condition, which is generally 200–500 ms in HVDC systems [18]. In the above proposed protection, the used high-frequency transient voltage is a fast-decay signal. Therefore, the

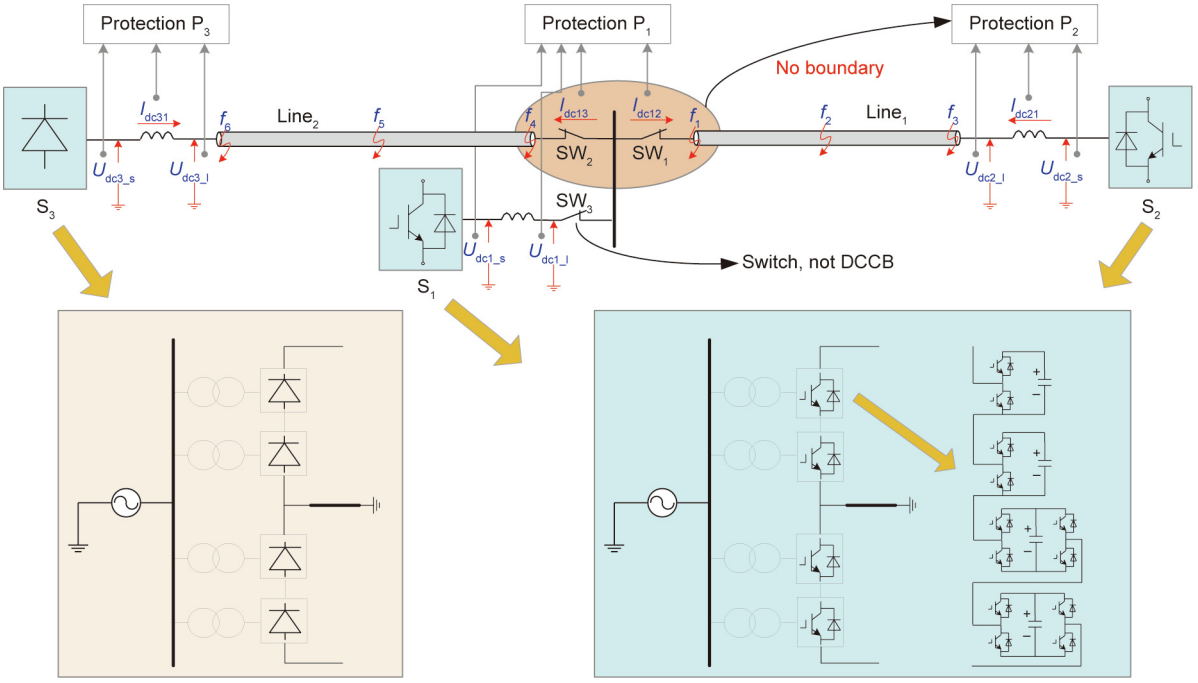

Fig. 1. Typical topology of a three-terminal hybrid HVDC transmission system. S_1, S_2, S_3: converter stations; SW_1, SW_2, SW_3: switches; f_1–f_6: faults; U_{dc1_s}, U_{dc2_s}, U_{dc3_s}: the DC voltage at the station side of the reactor at stations S_1, S_2, S_3, respectively; U_{dc1_l}, U_{dc2_l}, U_{dc3_l}: the DC voltage at the line side of the reactor at stations S_1, S_2, S_3, respectively; I_{dc31}: the DC current at S_3 output; I_{dc13}: the DC current from bus to $Line_2$; I_{dc12}: the DC current from bus to $Line_1$; I_{dc21}: the DC current at S_2 output; DCCB: DC circuit breaker.

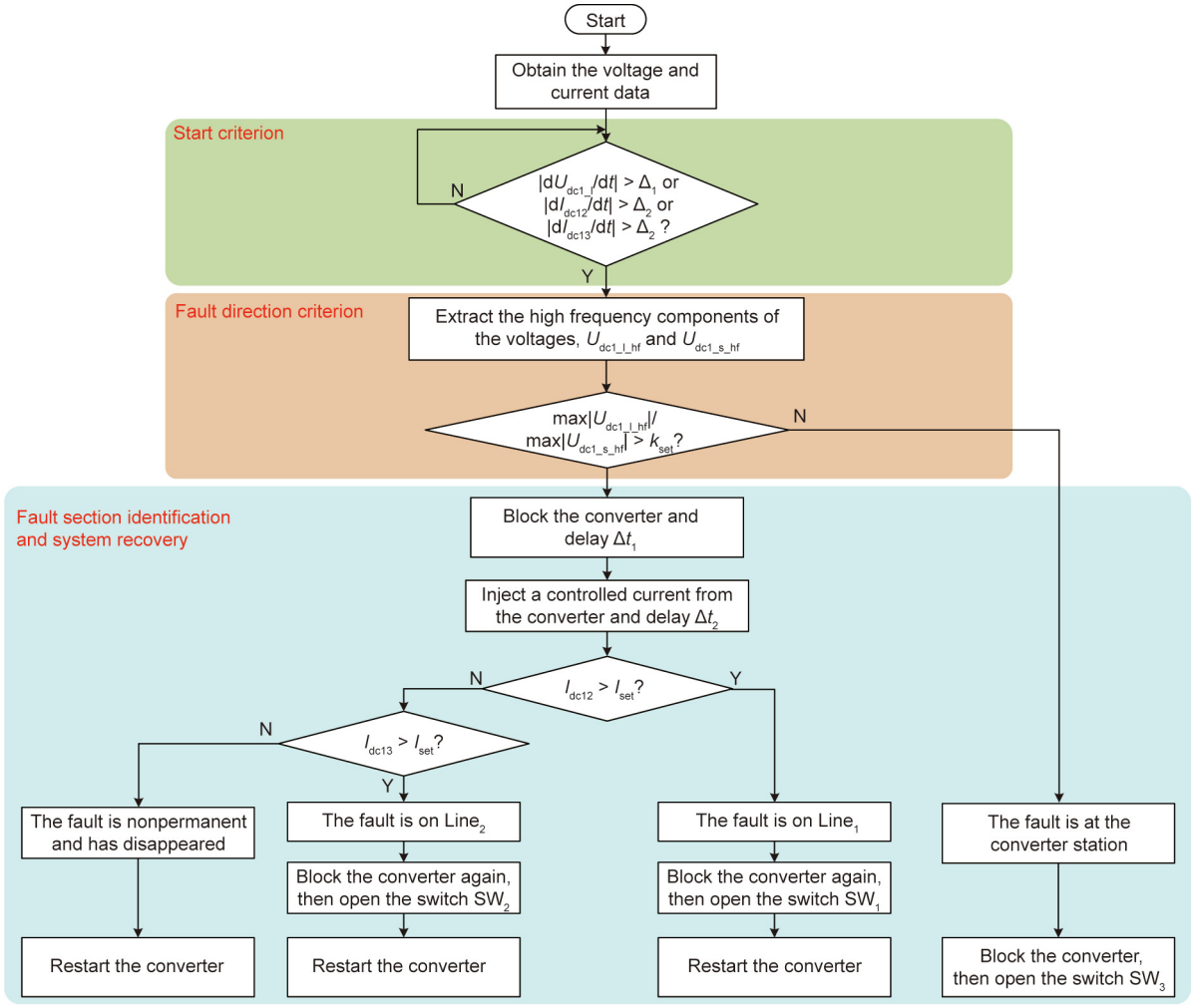

Fig. 2. Flowchart of the proposed protection strategy for the multi-terminal hybrid HVDC system.

wavelet transform is applied to extract this high-frequency transient voltage because the wavelet transform has an outstanding time-domain resolution in the high-frequency range [8,9]. In addition, the theoretical basis and corresponding verification of the fault direction criterion based on $\max|U_{dc1\_l\_hf}|/\max|U_{dc1\_s\_hf}|$, which is used to determine on which side of the reactor the fault occurs, has been studied in Refs. [8] and [10], and is thus not discussed in detail in this study.

In addition, during the shutdown of the converter, the proposed protection may operate by mistake, because the rate of change of voltage and current will also be very large. However, it should be noted that, in the hybrid HVDC system, the shutdown of the converter is realized by cooperation between different converter stations, which implies that the shutdown signal will be communicated between all the converter stations [19]. Therefore, this signal can also be sent to the protection. When the protection receives the converter shutdown signal, it will be blocked for a period of time to prevent the protection from operating by mistake.

3.2. Control strategy of current active injection

In the above proposed protection strategy, the core concept is to use a controlled current from the converter to distinguish the fault line ($Line_1$ or $Line_2$), and to identify the fault property (to determine whether the fault has disappeared or not). In this section, the control strategy of the converter to inject a controlled current is introduced (taking the converter station S_1 for instance), as shown in Fig. 3.

According to the working principle of the hybrid MMC, all the IGBTs in the FBSMs and HBSMs are blocked to eliminate the fault current when the DC fault is detected. After a delay time Δt_1 for insulation recovery, the switches connected in parallel with the starting resistors, which are installed at the converter side in pactical engineering, are opened to connect the resistors into the system. Then, the IGBT T_1 in each FBSM is turned on, as shown in Fig. 3.

Based on the above control strategy, the operation state of the hybrid MMC is the same as that of an uncontrolled rectifier. Therefore, the AC-side source will feed a current to the AC side when the DC fault point still exists. Moreover, during this period, starting resistors (R_{lim}) with values of several thousands of ohms at the AC side of the converter are connected, so the current injected to the DC side can be limited to a controlled level, such that it will not damage the devices in the DC system.

Furthermore, if the fault is on $Line_1$, $I_{dc12} > 0$ and $I_{dc13} = 0$ (ignoring the line capacitor current), while if the fault is on $Line_2$, $I_{dc12} = 0$ and $I_{dc13} > 0$. Differently, if the fault point has disappeared, $I_{dc12} = 0$ and $I_{dc13} = 0$. Therefore, the criterion for fault line discrimination and fault property identification can be designed as

$$\begin{cases} I_{dc12} > I_{set} \text{ the fault is on Line}_1 \\ I_{dc13} > I_{set} \text{ the fault is on Line}_2 \\ I_{dc12} \le I_{set} \text{ and } I_{dc13} \le I_{set} \text{ the fault has disappeared} \end{cases} \quad (1)$$

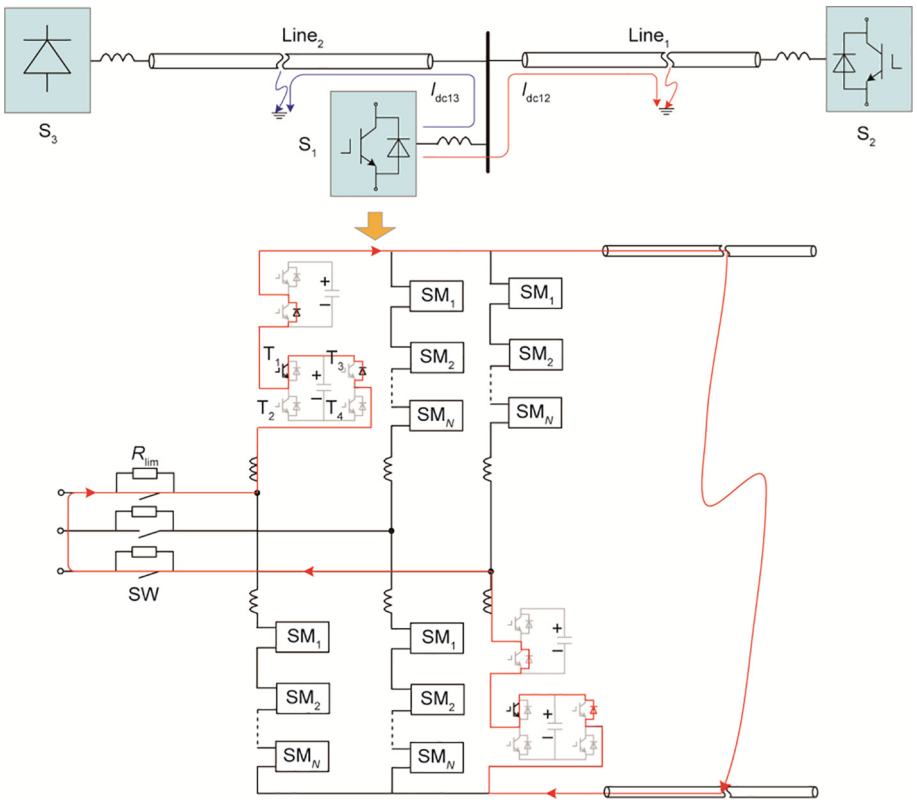

Fig. 3. Control strategy of the converter to inject a controlled current. R_{lim}: starting resistor; SW: switch; T_1, T_2, T_3, T_4: IGBT modules; SM_1–SM_N: sub-modules.

It should be noted that, owing to the distribution capacitors of the transmission line, at the initial stage of the current injection, a charging current will also occur on $Line_2$ when the fault is on $Line_1$, and it will occur on $Line_1$ when the fault is on $Line_2$. And this charging current will occur on $Line_1$ and $Line_2$ when the fault has disappeared. Therefore, the delay time Δt_2 is introduced before the criterion to guarantee that the charging current for the line capacitor has disappeared.

In addition, in the above content, the hybrid MMC consisting of the FBSMs and HBSMs is discussed as an example. In fact, for other types of hybrid MMCs using different self-eliminating sub-modules, such as clamp double sub-modules (CDSMs) and self-blocking sub-modules (SBSMs), the proposed active injection control strategy is also suitable. For example, for the hybrid MMC consisting of HBSMs and CDSMs as shown in Fig. 4(a), the IGBT T_5 in each CDSM is turned on during the active injection period. Therefore, the hybrid MMC operates as an uncontrolled rectifier to inject a controlled current to the DC side, similar to the condition shown as Fig. 3. Fig. 4(b) shows the current flowing path during the active injection period under the condition where SBSMs are applied. Similarly, with the

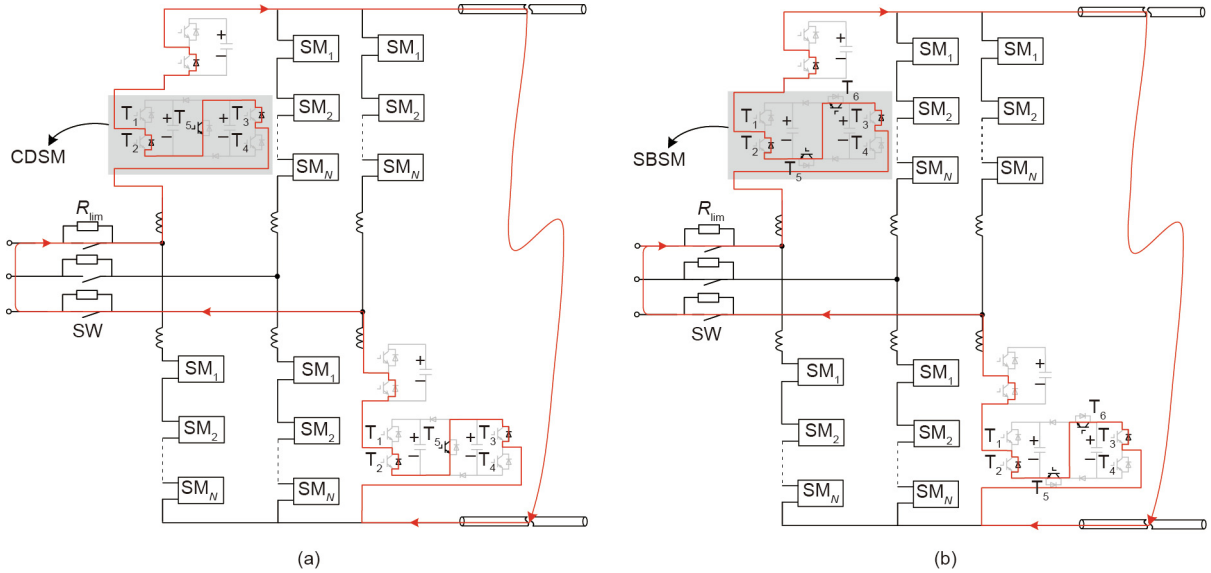

Fig. 4. Applicability of the designed active current injection control strategy under the condition with different kinds of self-eliminating sub-modules: (a) hybrid MMC consisting of CDSMs and HBSMs, and (b) hybrid MMC consisting of SBSMs and HBSMs.

IGBTs T_5 and T_6 turned on, the hybrid MMC also operates as an uncontrolled rectifier to inject a controlled current.

3.3. Cooperation with protection at other station terminals

As mentioned above, the protection strategy proposed in Section 3.1 is configured at station S_1 in the three-terminal hybrid HVDC system shown in Fig. 1. The protections at other two station terminals, namely protections P_2 and P_3, can be much simpler.

For the protections P_2 and P_3, the steps (1) and (2) in Section 3.1 are also executed. In other words, after the DC fault occurs, the protection P_2 and protection P_3 can also be started quickly. Then, the fault direction criterion based on the ratio of transient voltages at two sides of the reactor, that is, $\max|U_{dc2\_l\_hf}|/\max|U_{dc2\_s\_hf}|$ for P_2 and $\max|U_{dc3\_l\_hf}|/\max|U_{dc3\_s\_hf}|$ for P_3, is started to determine at which side of the reactor the fault occurs. If the fault is identified at the station side, the corresponding converter station is blocked, and the protection is ended. Differently, if the fault is identified at the DC side of the reactor, the fault current is eliminated by blocking the converter, which will be restarted when the line voltage recovers (described as follows).

For the protection P_3, if the local line voltage does not recover (e.g., $U_{dc3\_l} \leq 0.8U_{dcN}$, U_{dcN} represents the rated DC voltage), the converter S_2 will not be restarted all the time. Differently, for the protection P_2, if the local line voltage U_{dc2_l} does not recover for a delay time Δt_4, further operations will be carried out. According to the working principle of the protection strategy proposed in Section 3.1, only two conditions will cause the line voltage at S_2 terminal (U_{dc2_l}) to not recover during the delay time Δt_4: ① The DC fault occurs on $Line_1$, and the switch SW_1 has been opened; and ② the fault occurs in station S_1, and the switch SW_3 has been opened.

To distinguish between the above two conditions, the converter station S_2 will be controlled to inject a limited current. If the measured current $I_{dc21} > I_{set}$, it indicates that the fault is on $Line_1$, and the station S_2 should be re-blocked. If the current $I_{dc21} \leq I_{set}$, it indicates that the fault is not on $Line_1$ (i.e., it belongs to condition ②), and the converter should be restarted.

With the proposed protection strategy and corresponding cooperation strategy, the DC fault line can be distinguished (for permanent fault) and recovered (for nonpermanent fault) only according to the local information, which means that the communication is no longer required.

3.4. Threshold value selection

For engineering applications, the selection of the threshold values used in the proposed protection should be determined, and this is discussed in this section.

(1) Threshold values of the starting criterion: In the proposed protection, the rates of change of the DC voltage and DC currents are used to distinguish the fault condition and normal operation condition, and then start the protection. Therefore, the threshold value of Δ_1 should be larger than $|dU_{dc1\_l}/dt|$ during normal operation, and smaller than that under the weakest fault (remote high-resistance fault). Similarly, the value of Δ_2 should be larger than $|dI_{dc12}/dt|$ (or $|dI_{dc13}/dt|$) during normal operation, and smaller than that under the weakest fault. In engineering practice, the above threshold values should be determined according to the simulation results.

(2) Threshold value of the fault direction criterion: In the proposed protection, the fault direction criterion based on $\max|U_{dc1\_l\_hf}|/\max|U_{dc1\_s\_hf}|$ is used to identify the fault direction, that is, on which side of the reactor the fault occurs. According to Refs. [8] and [10], when the fault occurs on the line side of the reactor, the value of $\max|U_{dc1\_l\_hf}|/\max|U_{dc1\_s\_hf}|$ is larger than 1, while it is smaller than 1 when the fault occurs on the station side of the reactor. In the proposed protection, the reliability coefficient k_{set} is introduced to improve the operation reliability of the direction criterion. Generally, the selection of k_{set} is an empirical value, which is a little larger than 1 (e.g., 1.2).

(3) Threshold value of the fault section identification: According to the analysis in Section 3.2, during the active injection period, the DC line current is equal to zero if the fault has disappeared or is not on this line, while the DC line current is greater than zero if the fault point still exists. Therefore, the threshold value I_{set} can be very small, and only help in preventing the influence of measurement error and communication error.

(4) Threshold values of the delay times (Δt_1–Δt_3): In the proposed protection, the delay time Δt_1 is introduced for insulation recovery of the fault line, which is generally 200–500 ms in HVDC systems [18].

As analyzed above, the delay time Δt_2 is introduced to prevent the influence of the line-capacitor charging current under the condition that the fault has disappeared. During the active injection period, the converter operates as an uncontrolled rectifier. If the fault is still on the line, the DC current fed from the AC side will occur again, as shown by the blue curve in Fig. 5.

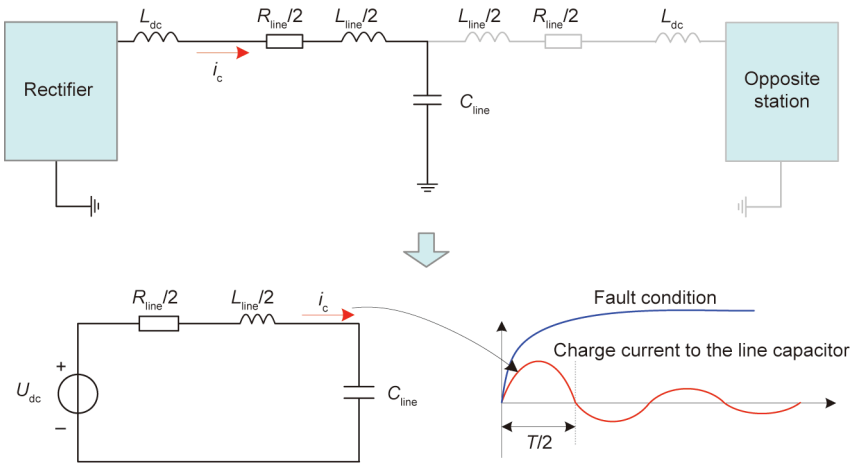

Fig. 5. Charge current to the line capacitor when the fault has disappeared or is not on this line. R_{line}: the equivalent resistance of the line; C_{line}: the equivalent capacitance of the line; L_{line}: the equivalent inductance of the line; U_{dc}: output DC voltage of the converter; T: time for one cycle; L_{dc}: value of inductor at converter DC output; i_c: transient charge current.

Differently, if the fault has disappeared or is not on this line, the steady-state DC current is zero, but there will be a transient charge current to the line capacitor, as shown by the red curve in Fig. 5. According to the equivalent circuit in Fig. 5, this transient charge current can be expressed as

$$i_c = \frac{2U_{dc}}{\omega(L_{line}+2L_{dc})} e^{-\sigma t} \sin \omega t \quad (2)$$

where $\sigma = R_{line}/(2L_{line})$; $\omega = \sqrt{(2/(L_{line}C_{line}) - \sigma^2)}$; R_{line}, L_{line}, and C_{line} represent the equivalent resistance, inductance, and capacitance of the line, respectively; U_{dc} is the output DC voltage of the converter (in the uncontrolled rectifier operation mode); L_{dc} is the value of inductor at converter DC output; and i_c is the transient charge current. As shown in Fig. 5, during the first half cycle ($T/2$), the charge current is a positive value, which may confuse the fault section and fault property identification, because the DC current during the condition where the fault still exists is also a positive value. However, after the first half cycle ($T/2$), the charge current will be a very small value or a negative value (in the subsequent half cycle). Therefore, the delay time Δt_2 should be larger than $T/2$, that is,

$$\Delta t_2 > \pi \Big/ \sqrt{\frac{2}{(L_{line}+2L_{dc})C_{line}} - \left(\frac{R_{line}}{2L_{line}}\right)^2} \quad (3)$$

For the protection P_1, the R_{line}, L_{line}, and C_{line} values of the longer line should be used to determine Δt_2, because the longer line has a larger L_{line} and C_{line}, which indicates a longer charge period.

In addition, the delay time Δt_3 should guarantee that the protection installed at station S_1 (protection P_1) has completed the corresponding operation. Therefore, Δt_3 should be larger than $\Delta t_2 + t_s + t_{wave\_dif}$, where t_s is the operation time of the switch and t_{wave_dif} is the initial-wave-arrival time difference between the protection P_1 and protection P_2. Furthermore, Δt_3 should also include the time for the DC voltage recovery.

4. Simulation case study

As shown in Fig. 1, the three-terminal hybrid HVDC transmission system is built based on power systems computer aided design (PSCAD)/electromagnetic transients including DC (EMTDC), whose parameters are listed in Table 1. In the built model, the station S_1 uses the LCC, while the stations S_2 and S_3 use the hybrid MMCs (hybrid of the HBSMs and FBSMs). In addition, the frequency-dependent model is used for the DC overhead lines. To verify the working principle and superiority of the proposed protection, the performances of the protection P_1, P_2, and P_3 with the sampling rate of 10 kHz are observed under different fault conditions. As explained in Section 3.4 and the parameters of the simulated model, the delay times Δt_1, Δt_2, and Δt_3 are set as 200, 10, and 50 ms, respectively. The value of k_{set} used in the fault direction criterion is set as 1.2. The threshold value I_{set} is set as 0.3 kA. In addition, it should be noted that the starting criterion based on the rate of change of voltage and the rate of change of current is a typical starting criterion used in the DC protection, and is thus not discussed in the simulation owing to space constraints.

4.1. Applicability of traditional single-ended protections in multi-terminal hybrid HVDC system

At present, the traveling-wave based protection, rate of change of voltage (ROCOV)-based protection or transient-voltage based protection is generally used as the primary protection in HVDC systems. In this section, the metallic pole-to-ground faults at f_1 and f_4 are set to happen at t = 6.3 s respectively. The performance of the protection P_2 is observed as shown in Fig. 6, to verify the applicability of the traditional single-ended DC protections in the multi-terminal hybrid HVDC system.

Table 1
Parameters of three-terminal hybrid HVDC system.

Parameter	Value
Rated DC voltage (S_1–S_3) (kV)	±770, ±780, ±800
Rated AC voltage (S_1–S_3) (kV)	525, 525, 535
DC exit reactor (S_1–S_3) (mH)	75, 75, 150
Rated power (S_1–S_3) (MVA)	3 132, 5 100, 9 720
Arm reactor (S_1–S_2) (mH)	61.2, 41.2
SM capacitor (S_1–S_2) (μF)	12 000, 18 000
SM number (S_1–S_2) (per arm)	210, 210
Length of the line ($Line_1$–$Line_2$) (km)	542, 908

Fig. 6(c) shows the simulation results of the backward voltage traveling waves observed at the protection P_2 respectively after the fault f_1 and f_4. As discussed above, the traveling-wave based protection primarily uses the amplitude of the voltage traveling wave to distinguish the internal and external faults. However, as shown in Fig. 6(c), for protection P_2, the observed voltage traveling wave after fault f_1 is almost the same as that after fault f_4. This is because there is no boundary between $Line_1$ and $Line_2$, and the fault points f_1 and f_4 are the same point in terms of space. This indicates that the single-ended traveling-wave based protection cannot distinguish the internal fault and external fault reliably in

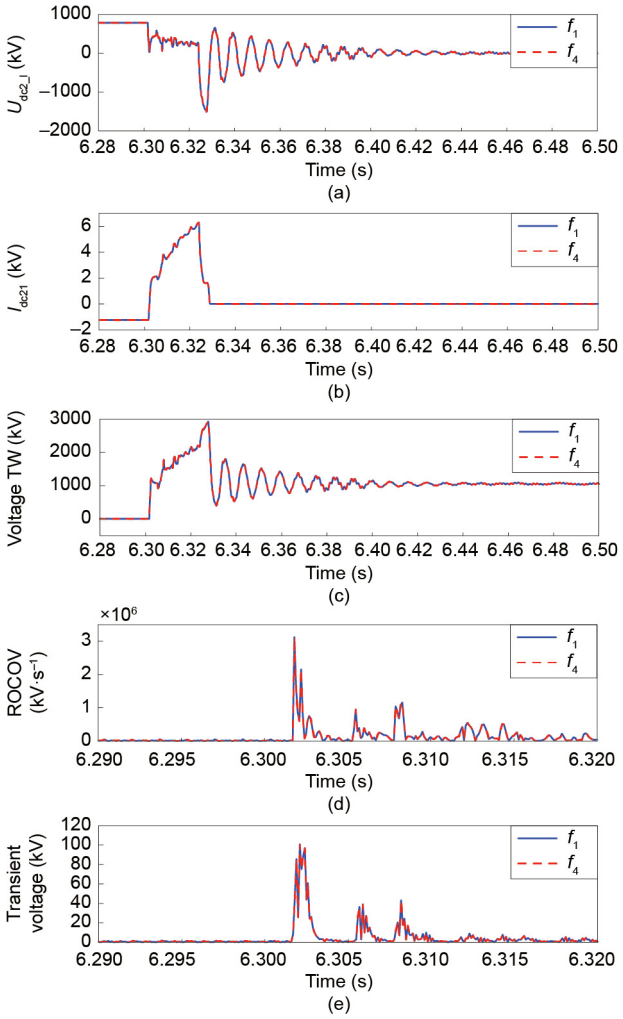

Fig. 6. Performances of the traditional single-ended DC protections after the faults f_1 and f_4 in the multi-terminal hybrid HVDC system: (a) DC voltage U_{dc2_l}, (b) DC current I_{dc21}, (c) voltage traveling wave (TW), (d) ROCOV, and (e) transient voltage.

the multi-terminal hybrid HVDC system, owing to the absence of the boundary element at the line end. Similarly, as shown in Figs. 6(d) and (e), the ROCOV based protection and transient-voltage based protection are also not suitable for the multi-terminal hybrid HVDC system.

4.2. Performance of proposed protection strategy

In this section, the DC faults at f_1 and f_2 are set to happen respectively, to show how the proposed protection strategy distinguishes the fault line without the boundary.

(1) Fault f_1:

In this case, the fault f_1 is set to happen at t = 6.3 s. Fig. 7 shows the corresponding simulation results. As shown in Fig. 7(a), after the DC fault f_1, the ratio of $\max|U_{dc1\_l\_hf}|/\max|U_{dc1\_s\_hf}|$ is 2.99, which is larger than the threshold value 1.2. Therefore, the fault is identified as the line-side fault by the protection P_1. In addition, the active injection control strategy is put into operation for converter S_1 after the delay time Δt_1 (at approximately t = 6.502 s). As shown in Fig. 7(b), after the active injection, the DC current on $Line_1$, namely I_{dc12}, is larger than the threshold value I_{set} (0.3 kA) after the delay time Δt_2. Therefore, $Line_1$ is distinguished as the fault line, and is thus cut off by the switch SW_1. Subsequently, the station S_1 is restarted to build the DC voltage. Therefore, the line voltage at the station S_3 terminal, that is, U_{dc3_l}, also quickly increases above the threshold value 640 kV, as shown in Fig. 7(e). The protection P_3 measures the recovery of U_{dc3_l}, and the station S_3 is restarted. At the station S_2, the line voltage (U_{dc2_l})

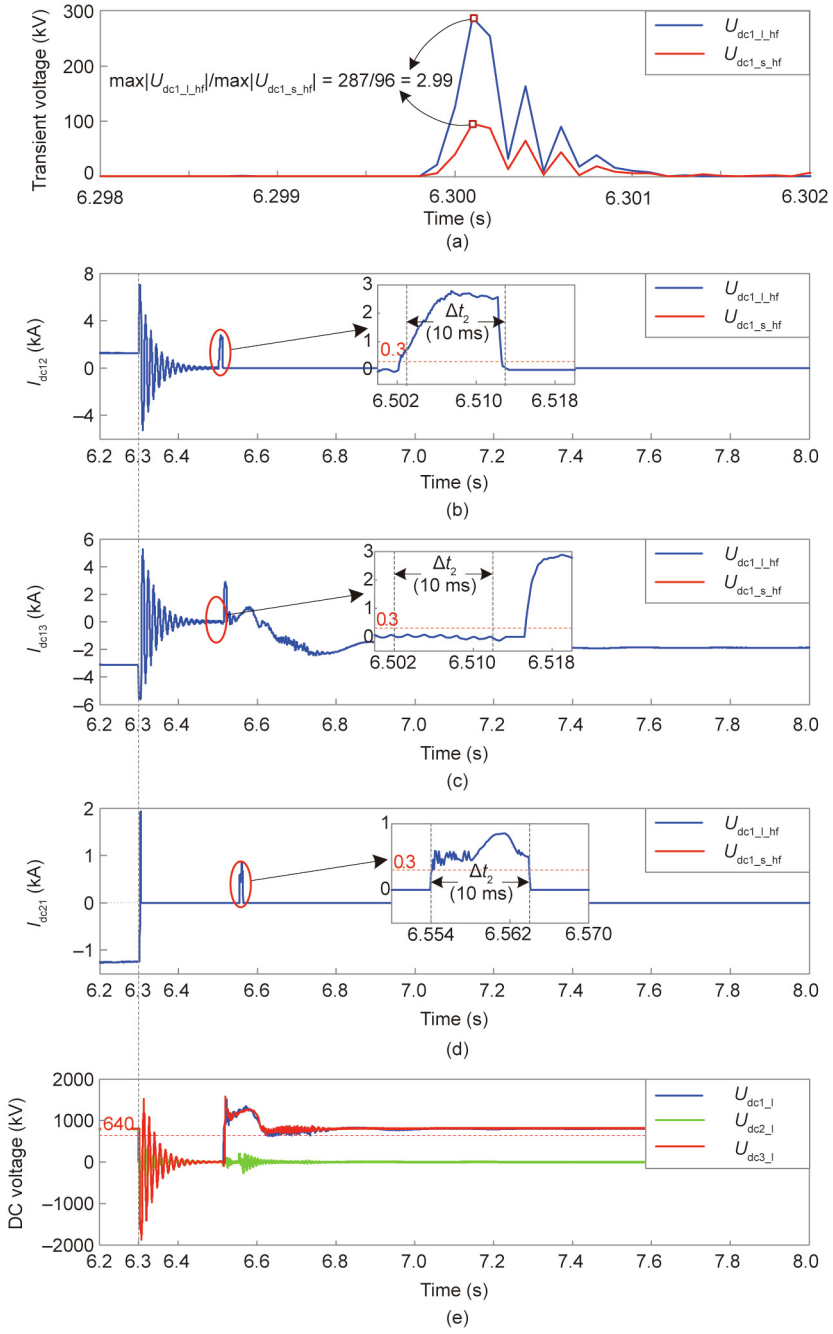

Fig. 7. Performance of the proposed protection strategy after the metallic fault f_1: (a) transient voltages, (b) DC current I_{dc12}, (c) DC current I_{dc13}, (d) DC current I_{dc21}, and (e) DC voltages.

always does not recover, and the DC current (I_{dc21}) increases to exceed the threshold value during the active injection (Fig. 7(d)). Therefore, the protection P_2 determines that the fault is on $Line_1$, and the station S_2 is not restarted, as shown in Fig. 7(e).

In addition, it should be noted that, during the active current injection period, the injected current remains at a controlled level (below the rated DC current, as shown in Figs. 7(b) and (d)). This is because the large starting resistor on the AC side of the converter is connected into the system during this period, and the injected current is limited effectively.

(2) Fault f_4:

In this case, the fault f_4 is set to happen at t = 6.3 s. Fig. 8 shows the corresponding simulation results. Similarly, the fault is identified as DC-side fault reliably, as shown in Fig. 8(a). However, differently, after the active injection, the DC current on $Line_1$ (I_{dc12}) is not larger than the threshold value I_{set}, while the DC current on $Line_2$ (I_{dc13}) exceeds I_{set}. Therefore, $Line_2$ is distinguished as the fault line, which is cut off by the switch SW_2. Subsequently, the station S_1 is restarted to build the DC voltage. Thus, the protection P_2 measures the recovery of the line voltage (U_{dc2_l}), as shown in Fig. 8(e), and the station S_2 is also restarted. In addition, the protection P_3 cannot monitor the recovery of the line voltage (U_{dc3_l}) and therefore the station S_3 is not restarted.

The above cases verify that the proposed protection strategy can distinguish the fault line reliably and realize the fast recovery of the healthy network, in the multi-terminal hybrid HVDC transmission system. In addition, it should be noted that, owing to the application of the starting resistor during the active injection

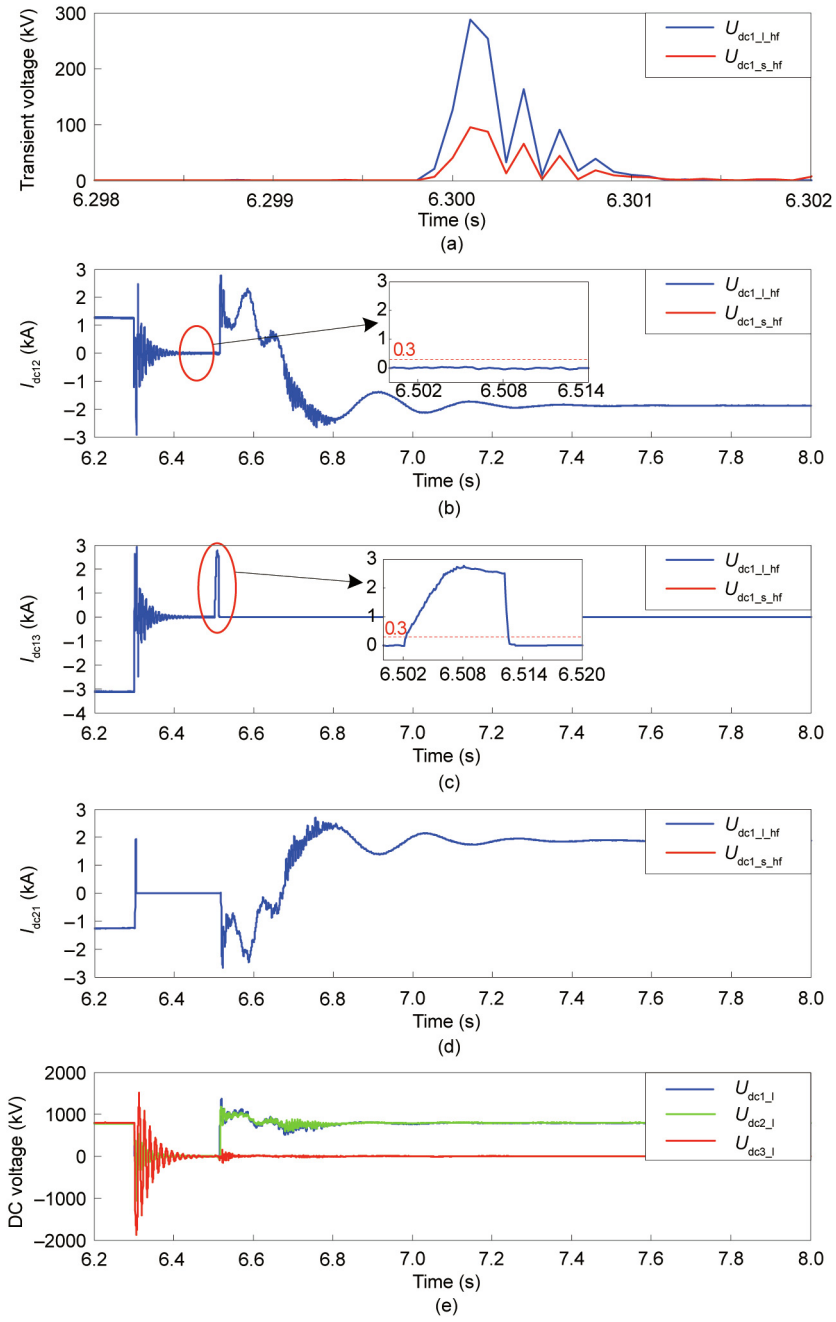

Fig. 8. Performance of the proposed protection strategy after the metallic fault f_4: (a) transient voltages, (b) DC current I_{dc12}, (c) DC current I_{dc13}, (d) DC current I_{dc21}, and (e) DC voltages.

period, the injected current is limited at an acceptable range, thus causing no damage to the system.

4.3. Robustness of the proposed protection strategy

In this case, the performances of the proposed protection strategy after the faults at different positions are observed. As shown in Figs. 9 and 10, either after the fault f_2 at the middle of $Line_1$ or after the fault f_3 at the end of $Line_1$ (for the protection P_1), the proposed protection strategy distinguishes the fault line ($Line_1$) and recovers the healthy network reliably. This indicates that the proposed protection can reliably operate after the faults at different positions. In addition, in the case of the fault f_3, a 300 Ω transition resistor is introduced. As shown in Fig. 10, the correct operation verifies that the proposed protection has strong ability against high transition resistance.

5. Conclusions

DC protection is an important technique for the engineering application of multi-terminal hybrid HVDC transmission systems. However, the typical single-ended protections used in LCC-HVDC and VSC-HVDC systems are not suitable for multi-terminal hybrid HVDC systems, owing to the absence of the boundary element at the line end. This study proposes a novel single-ended protection strategy suitable for multi-terminal hybrid HVDC transmission systems. The proposed protection uses the transient voltage to identify the fault direction (DC side or converter side), then

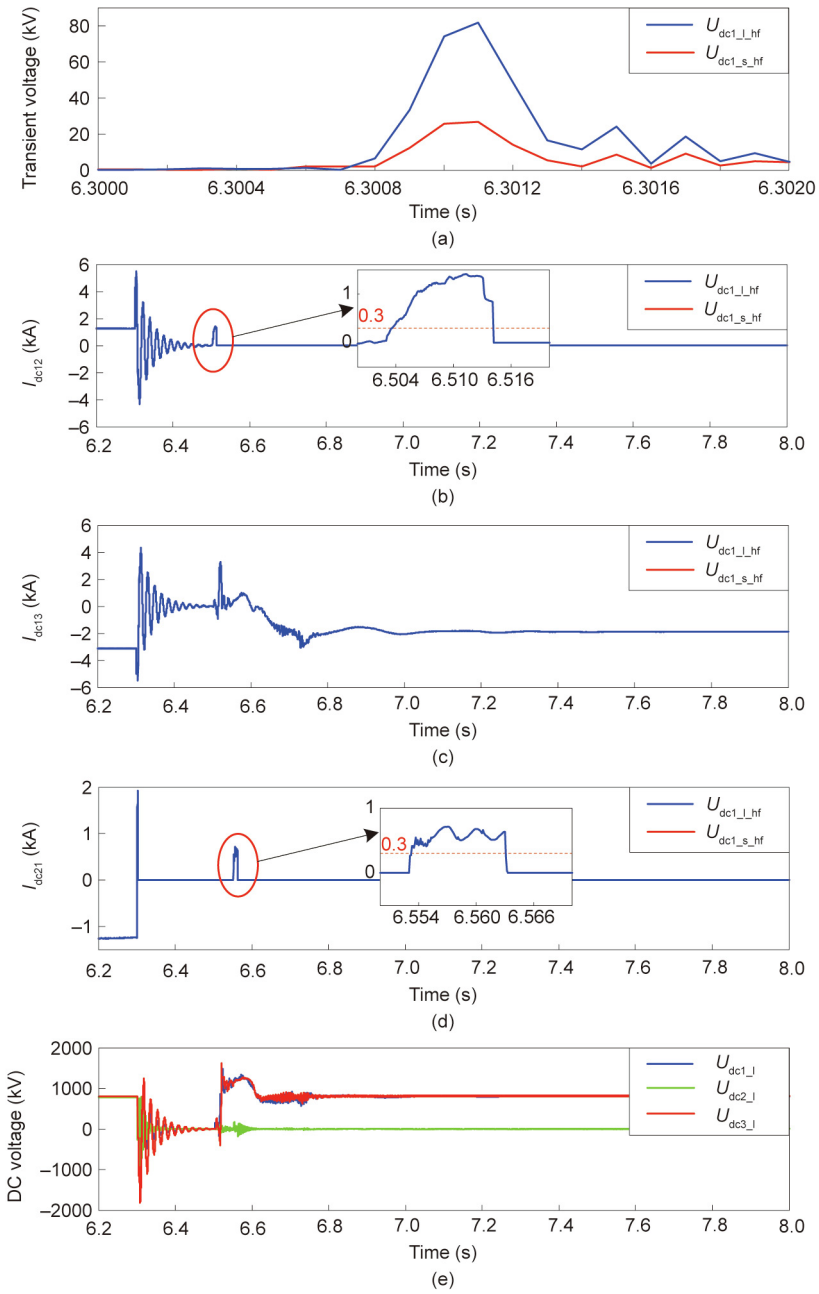

Fig. 9. Performance of the proposed protection strategy after the metallic fault f_2: (a) transient voltages, (b) DC current I_{dc12}, (c) DC current I_{dc13}, (d) DC current I_{dc21}, and (e) DC voltages.

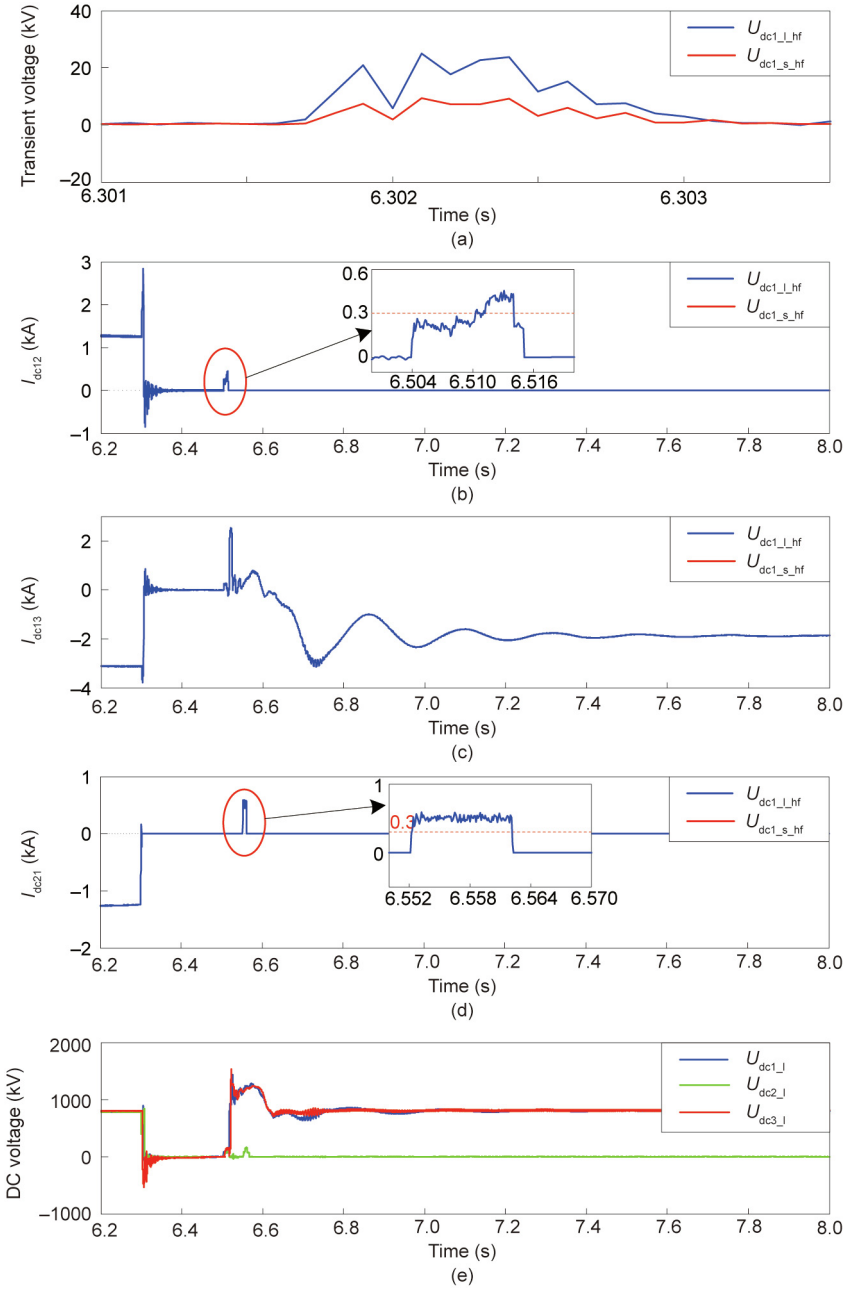

Fig. 10. Performance of the proposed protection strategy after the fault f_3 with a 300 Ω transition resistance: (a) transient voltages, (b) DC current I_{dc12}, (c) DC current I_{dc13}, (d) DC current I_{dc21}, and (e) DC voltages.

distinguishes the fault line according to the active injected current. Compared with the single-ended protections used in LCC-HVDC and VSC-HVDC systems, the proposed protection can reliably and correctly operate without the line boundary. Moreover, the communication is not required by the proposed protection, and the investment can thus be reduced when compared with pilot protections (such as the current differential protection).

Compliance with ethics guidelines

Yuping Zheng, Jiawei He, Bin Li, Tonghua Wu, Wei Dai, and Ye Li declare that they have no conflict of interest or financial conflicts to disclose.

References

[1] Kalair A, Abas N, Khan N. Comparative study of HVAC and HVDC transmission systems. Renew Sustain Energy Rev 2016;59:1653–75.
[2] Ooi BT, Wang X. Boost-type PWM HVDC transmission system. IEEE Trans Power Deliv 1991;6(4):1557–63.
[3] Teeuwsen SP, editor. Modeling the Trans Bay cable project as voltage-sourced converter with modular multilevel converter design. In: Proceedings of the IEEE Power and Energy Society General Meeting; 2011 Jul 24–28; Detroit, MI, USA. New York: IEEE; 2011. p. 1–8.
[4] Haleem NM, Rajapakse AD, Gole AM, Fernando IT. Investigation of fault ride-through capability of hybrid VSC-LCC multi-terminal HVDC transmission systems. IEEE Trans Power Deliv 2019;34(1):241–50.
[5] Wang Y, Zhao W, Yang J, Wang N, Lu Y, Li H. Hybrid high-voltage direct current transmission technology and its development analysis. Autom Electr Power Syst 2017;41(7):156–167. Chinese.
[6] Wu J, Li H, Wang G, Liang Y. An improved traveling-wave protection scheme for LCC-HVDC transmission lines. IEEE Trans Power Deliv 2017;32(1):106–16.

[7] Ma Y, Li H, Wang G, Wu J. Fault analysis and traveling-wave-based protection scheme for double-circuit LCC-HVDC transmission lines with shared towers. IEEE Trans Power Deliv 2018;33(3):1479–88.
[8] Li B, Li Ye, He J, Wen W. A novel single-ended transient-voltage-based protection strategy for flexible DC grid. IEEE Trans Power Deliv 2019;34 (5):1925–37.
[9] De Kerf K, Srivastava K, Reza M, Bekaert D, Cole S, Van Hertem D, et al. Wavelet-based protection strategy for DC faults in multi-terminal VSC HVDC systems. IET Gener Transm Distrib 2011;5(4):496–503.
[10] Liu J, Tai N, Fan C. Transient-voltage-based protection scheme for DC line faults in the multiterminal VSC-HVDC system. IEEE Trans Power Deliv 2017;32 (3):1483–94.
[11] Xiang W, Yang S, Xu L, Zhang J, Lin W, Wen J. A transient voltage-based DC fault line protection scheme for MMC-based DC grid embedding DC breakers. IEEE Trans Power Deliv 2019;34(1):334–45.
[12] Guo C, Liu B, Zhao C. A DC chopper topology to mitigate commutation failure of line commutated converter based high voltage direct current transmission. J Mod Power Syst Clean Energy 2020;8(2):345–55.
[13] Rao H, Hong C, Zhou B, Huang D, Xu S, Yao W, et al. Study on improvement of VSC-HVDC at inverter side of Wudongde multi-terminal UHVDC for the problem of centralized multi-Infeed HVDC. South Power Syst Technol 2017;11 (3):1–5. Chinese.
[14] Petino C, Heidemann M, Eichhoff D, Stumpe M, Spahic E, Schettler F. Application of multilevel full bridge converters in HVDC multiterminal systems. IET Power Electron 2016;9(2):297–304.
[15] Zhang J, Zhao C. The research of SM topology with DC fault tolerance in MMC-HVDC. IEEE Trans Power Deliv 2015;30(3):1561–8.
[16] Li R, Fletcher JE, Xu L, Holliday D, Williams BW. A hybrid modular multilevel converter with novel three-level cells for DC fault blocking capability. IEEE Trans Power Deliv 2015;30(4):2017–26.
[17] Qin J, Saeedifard M, Rockhill A, Zhou R. Hybrid design of modular multilevel converters for HVDC systems based on various submodule circuits. IEEE Trans Power Deliv 2015;30(1):385–94.
[18] Vinothkumar K, Segerqvist I, Johannesson N, Hassanpoor A. Sequential auto-reclosing method for hybrid HVDC breaker in VSC HVDC links. In: Proceedings of the 2016 IEEE 2nd Annual Southern Power Electronics Conference (SPEC); 2016 Dec 5–8; Auckland, New Zealand. New York: IEEE; 2016. p. 1–6.
[19] Guo XS, Zhou Y, Yang MJ, Yao WZ. Research on control scheme for single converter online entry/exit in dual-converter based VSC-HVDC. Power Syst Technol 2019;43(9):3393–8. Chinese.